New Sidewall Materials in Aluminum Reduction Cell

Yawei Li, Yibiao Xu

Nowadays the heat dissipating has to be reduced as far as possible in new electrolysis technology in order to meet the needs of energy saving in aluminum industry. Ledge-free sidewall is preferred as it potentially reduces the energy requirement of aluminum production and allows the use of larger anode that increase capacity and productivity of a cell of the same dimensions. Also the environmental impacts would be reduced significantly in combination with inert anodes and cathode application. However, the sidewalls are facing the extreme challenge because they will be in direct contact with oxidizing, corrosive and reducing environments for different zones in aluminum cell. This article gives an overview of the current status and latest progress of such ledge-free sidewall materials. Also, an attempt to develop novel composite materials based on MgO–$NiFe_2O_4$–TiO_2 and MgO–SnO_2–TiO_2 system for ledge-free sidewall have been made in our laboratory. Finally, some advices on the development of the ledge-free sidewall materials in future are proposed.

1 Introduction

It is well-known that the Hall-Héroult process is only industrially viable one to produce aluminum. Such an electrolysis based process includes the dissolution of commercial alumina into molten electrolyte, and reduction into aluminum at about 970 °C using carbon anodes. During this process molten aluminum is generated at the cathode, and the carbon anode is oxidized and consumed to produce 70–90 % CO_2 [1]. Meanwhile, in practical process, Si_3N_4 bonded SiC refractory has been chosen as the sidewall materials in aluminum reduction cell, on inner side of which a frozen ledge of electrolyte forms because of its high thermal conductivity [2–5]. In this case a large heat accounting for approximately 35 % of the total input energy has to transfer through the sidewalls [6–8], which is the reason for the low energy efficiency of 40–45 % in current Hall-Héroult process.

Nowadays it come to realize that such heat dissipating should be reduced as far as possible in new electrolysis technology in order to meet the needs of energy saving in aluminum industry [9, 10]. For example, once a high insulation layer was applied outside the sidewalls in new technology, there was ledge-free on inner side and the heat in the cell could be kept rather than removed, leading to a potentially 30–40 % energy savings. Such a ledge-free sidewall may also allow the use of larger anodes to increase the capacity and productivity of the same dimension cell [11]. Furthermore, if the combination of inert anodes and cathode were used in new technology, the environmental impacts would be reduced significantly. However, in that case the sidewall would be exposed directly to the oxidizing gas, corrosive electrolyte and reducing aluminum from the top to bottom causing significantly the reduction of the sidewall service life if Si_3N_4 bonded SiC materials were still used as sidelining [12–14]. An alternative approach to tackling these difficulties is to develop a new material as sidelining instead of the frozen ledge on the inner of the traditional sidewall [10]. However, the tough challenges to new sidewall material have to withstand all different surrounding environments in aluminum reduction cells.

In present paper, the requirements and structure design for ledge-free sidewall will be introduced, and then the state of the art for sidewall materials is reviewed. Following that MgO–$NiFe_2O_4$–TiO_2 and MgO–SnO_2–TiO_2, as candidate materials are presented on our research work. Finally, the development of new materials as sidewall is further proposed.

2 Requirements and structure design for ledge-free sidewall

The required properties of the ledge-free sidewall can be divided into physical, chemical as well as economical characteristics [16, 17], which are summarized as listed in Tab. 1. Based on the above criteria it is difficult to develop only a kind of material satisfying all the chemical requirements of the sidewall [9, 10], Mukhlis, et al. [9] have proposed multi-layer strategy and heat flux strategy to tackle the combining corrosive action on the different environments within the cell as illustrated in Fig. 1. Multi-layer strategy can be applied horizontally at gas, bath and metal zones where the different materials to be used can withstand each

Yawei Li, Yibiao Xu
The State Key Laboratory of Refractories and Metallurgy,
Wuhan University of Science and Technology,
430081Wuhan
China

Corresponding author: *Yawei Li*
E-mail: liyawei@wust.edu.cn

Keywords: sidewalls; $NiFe_2O_4$; SnO_2; composite spinel; electrolyte corrosion resistance, aluminum industry

Received: 20.04.2014
Accepted: 18.06.2014

Tab. 1 General selection criteria for an ideal ledge-free sidewall material

Physical requirements	Low electrical conductivity
	Low thermal conductivity
	High mechanical strength
	High thermal shock resistance
	Superior abrasion resistance to bath
	Low porosity
Chemical requirements	Not reactive to electrolyte and Al
	Low solubility in molten electrolyte and Al
	High oxidation resistance
	Not wetted by molten electrolyte and Al
Economical requirements	Low fabrication costs
	Ease of joining

zone mentioned above (Fig. 1a). In general, the interface of gas and bath zone as well as bath and metal zone shifts during the electrolysis process. Therefore, the appropriate horizontal multi-layer strategy is to use two kinds of materials, namely, one of them can withstand the gas and bath zone while the other is in the bath and metal zone. Similarly, multi-layer strategy can be applied vertically that one kind of material with high corrosion resistance is within the cell while the other one with low heat conductivity to maintain the heat balance of the cell applied outside (Fig. 1b). This strategy would not be available because only a kind of material as inside wall could not meet the requirements for three different environments.

The third strategy is recommended in Fig. 1c, which controls heat flux through bath zone to allow ledge formation on this zone while heat flux through the air and metal zone is minimized by incorporating air gaps or inserting low heat conductivity material into sidewall. In this case a certain amount of energy has to be dissipated through the sidewall, which make it difficult to achieve a potentially 30–40 % energy savings.

3 The state-of-the art for sidewall materials

Recently, the efforts have mainly focused on developing materials for both of the gas and bath zones where the sidewall is facing the most extreme challenge in these areas. $NiFe_2O_4$ and SnO_2 are in investigation for sidewall materials with respect to that these oxides have high stability in air and bath. In fact, these oxides are regarded as potential materials for inert anodes in aluminum reduction cell [16, 22, 23] which should possess the desirable properties similar to those of the sidewall materials except for high electrical conductivity.

3.1 Nickel ferrite as sidewall material

$NiFe_2O_4$ is of interest as novel sideling materials [11, 17, 22] due to its high resistance toward the electrolyte and oxygen [16, 19, 24], which could be used as a sidewall refractory, either as a bulk refractory or as part of a multi-refractory system. *Yan et al.* [24] studied the dynamic corrosion of nickel ferrite samples in molten bath with specimen rotation speed of 25 rpm. Specimen with higher porosity was associated with more serious bath infiltration. Besides, the extent of corrosion of the nickel ferrite could be lowered by using high alumina content as well as low NaF/AlF_3 molar ratios (CR). It was also proposed that the mechanism of corrosion involved grain boundary attack and therefore specimen with larger grain size had better corrosion resistance in the bath.

Downie [22] has also confirmed that nickel ferrite specimen with a larger grain size showed better performance than that of specimen with smaller grains in cryolite-based baths under static conditions. Besides, aluminum-rich oxide phase formed inside the specimens with Fe-Ni metal alloy at the surface of the corroded part. Similarly, Sekhar, et al. [25] observed the formation of a metallic phase by the immersion of nickel ferrite in molten cryolite. Nightingale, et al. [11] reported some larger Fe-Ni metallic particles in the residual bath and many smaller ones are scattered throughout the reaction zone after nickel ferrite was tested in cryolite bath containing 10 % alumina for 4 h (Fig. 2a). Grain boundaries were being attacked accompanying with the formation of aluminum rich phase in the grain boundaries (Fig. 2b), and grains separated from the bulk. And it suggested that additives in nickel ferrite spinel based materials could impart resistance to grain boundary penetration in combination with increasing the grain size. In addition, Olsen and Thonstad [26, 27] observed that a dense layer of about 50 µm formed at the surface

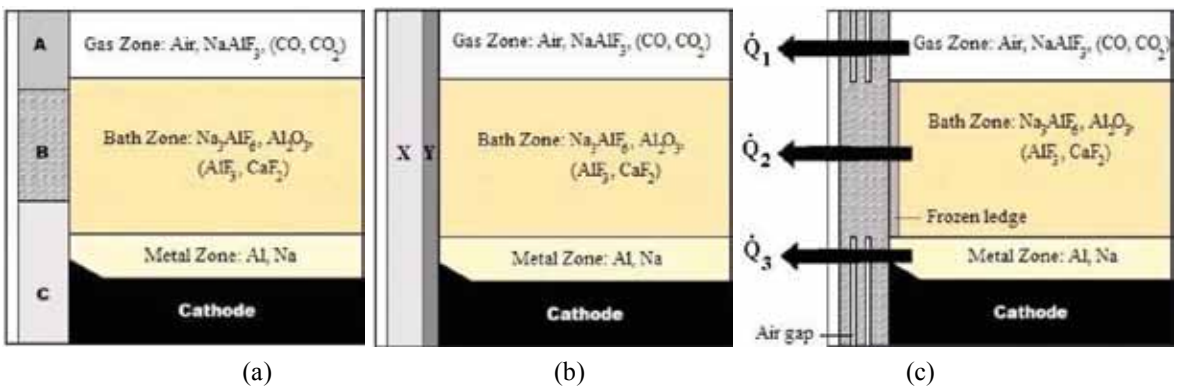

Fig. 1a–c Horizontal layer strategy (a), vertical layer strategy (b), and heat flux strategy (c)

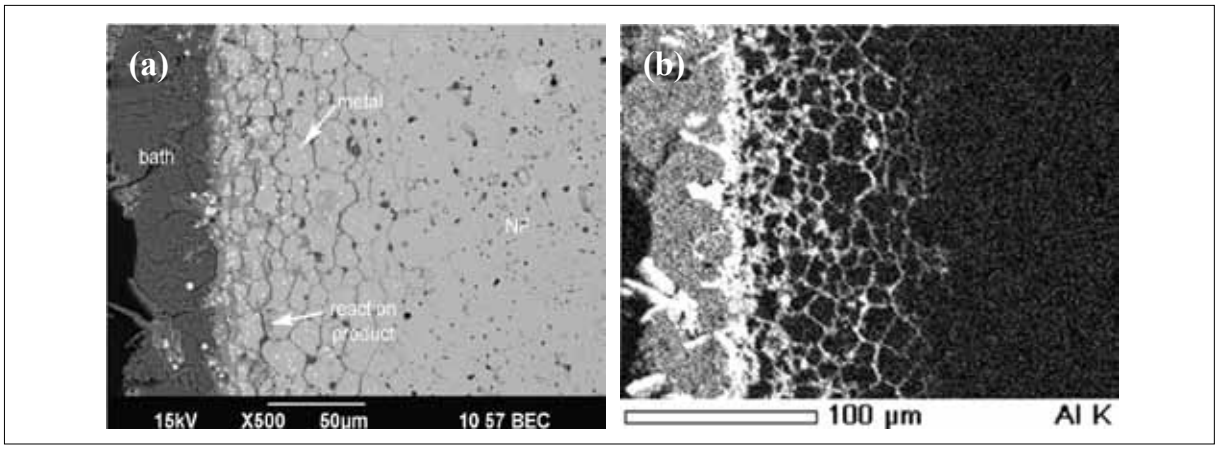

Fig. 2a–b Nickel ferrite after corrosion in 10 % alumina-cryolite bath at 980 °C for 4 h (a), and elemental map of Al for the same region (b)

of nickel ferrite based anodes after corroded in alumina-cryolite bath, which were composed of aluminates, such as $FeAl_2O_4$ and $NiAl_2O_4$, hindering further chemical corrosion in the molten electrolyte.

Overall, the extent of corrosion of the nickel ferrite in all the experiments above is quite small. Thus, nickel ferrite might be suitable to be applied in the gas zone and bath zone and unfit in the metalzone due to the dissolution of iron and nickel to aluminum as shown in Fig. 3 [10, 28].

3.2 SnO_2 as sidewall material

SnO_2 also demonstrates extremely low solubility in cryolite melt under oxidizing atmosphere [29–35], which may be another candidate material for sidelining. *Xiao et al.* [29] reported that the solubility of SnO_2 increased with decreasing Al_2O_3 concentration and increased with increasing temperature, and it showed a maximum at NaF/AlF_3 molar ratio (CR) of 3. Meantime, the solubility of SnO_2 was associated with oxygen partial pressure over the melts due to formation of divalent tin (Sn(II)) species. Xiao, et al. [30] also confirmed that high current densities led to serious corrosion of the anode specimens as well as low NaF/AlF_3 molar ratios and low alumina concentrations. Keller, et al. [32] pointed out that the electrolyte corrosion mechanism was mainly governed by solubility of SnO_2 ceramic and the mass transport condition. With respect to additives, Vecchio-Sadus, et al. [36] examined the performance of SnO_2 ceramic anodes doped with copper and antimony oxides in cryolite alumina melts. CuO additive could enhance the sinterability of the SnO_2 based ceramic [39].

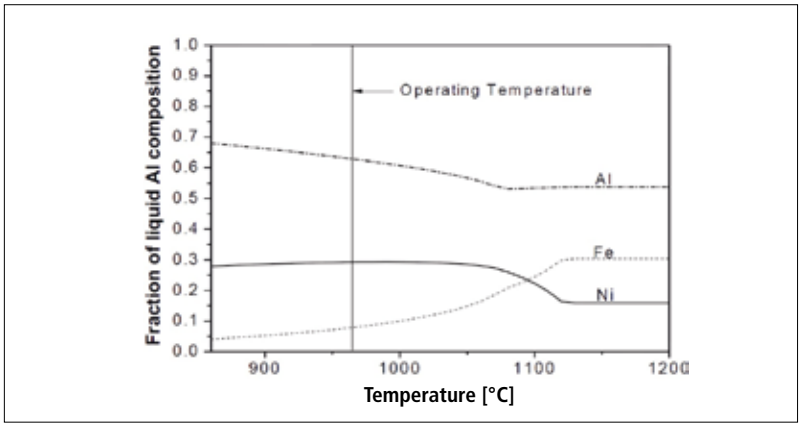

Fig. 3 Equilibrium calculations of 1 mol nickel ferrite and 10 mol aluminum at 860 – 1200 °C

However, after corrosion test, the Cu depletion zone appeared causing a subsequent decrease in mechanical strength of the ceramic [34, 35].

It is worth mentioning that though the pure SnO_2 materials obtained high chemical stability in molten electrolyte under the oxidizing atmosphere, they still can not be applied in the aluminum zone since it can be easily reduced into metal Sn [37].

3.3 Aluminate spinel as sidewall material

Jentoftsen, et al. reported some aluminate spinels, such as $FeAl_2O_4$ and $NiAl_2O_4$, also possess high chemical stability in the cryolite-alumina melts [38]. And Olsen and Thonstad [26] confirmed that the corrosion rate of nickel ferrite anodes in cryolite bath was reduced obviously when an aluminates spinels layer formed at the surfaces. Recently, Yan, et al. [10] prepared a series of aluminate spinels, including $NiAl_2O_4$, $MgAl_2O_4$ and $Ni_xMg_{(1-x)}Al_2O_4$ solid solutions, as candidate materials for the sidewalls. It revealed that the $NiAl_2O_4$ and $MgAl_2O_4$ spinels had good corrosion resistance toward the melts, with solubility of Ni from $NiAl_2O_4$ being 0,01 mass-% and Mg from $MgAl_2O_4$ being 0,07 mass-%. Interestingly, it was also found that the concentrations of Ni and Mg from the $Ni_{0,5}Mg_{0,5}Al_2O_4$ solid solution in the bath were lowered to 0,007 mass-% Ni and 0,05 mass-% Mg due to reduced activities of NiO and MgO in the spinel solid solution. It is deduced that the $Ni_{0,5}Mg_{0,5}Al_2O_4$ solid solution might be also more difficult to reduce by liquid Al and proposed that $(Ni,Mg)Al_2O_4$ solid solutions could be potentially promising materials for the ledge-free sidewalls.

4 Magnesia-based composite as sidewall material

In fact, magnesia based compositions could be candidates applied in the gas and bath zone due to ist good resistance to basic slags as well as low price [40]. The magnesia materials would not contaminate Al melt since the reaction products of MgO and

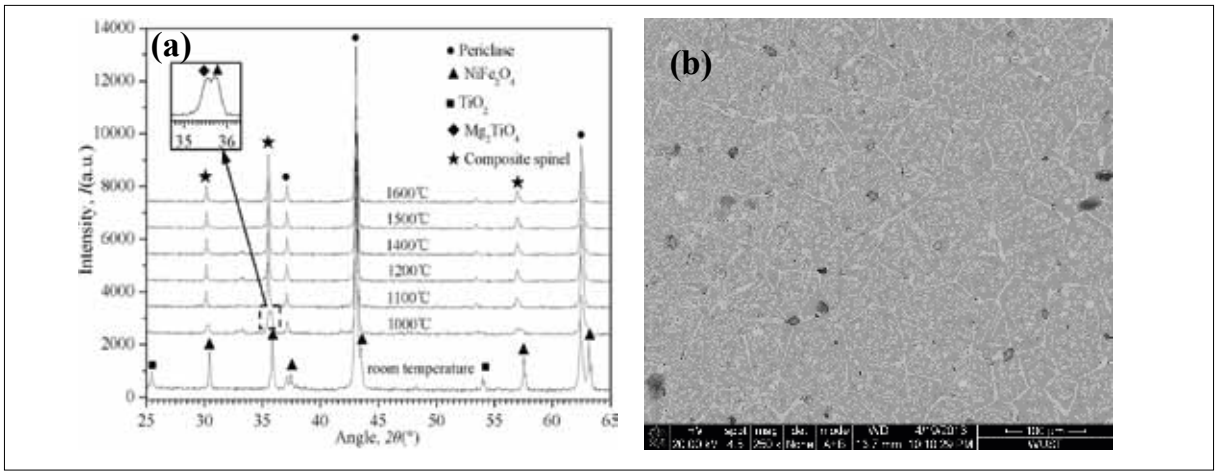

Fig. 4a–b XRD patterns of specimen MTN30 at various temperatures (a), and its micrograph fired at 1600 °C (b)

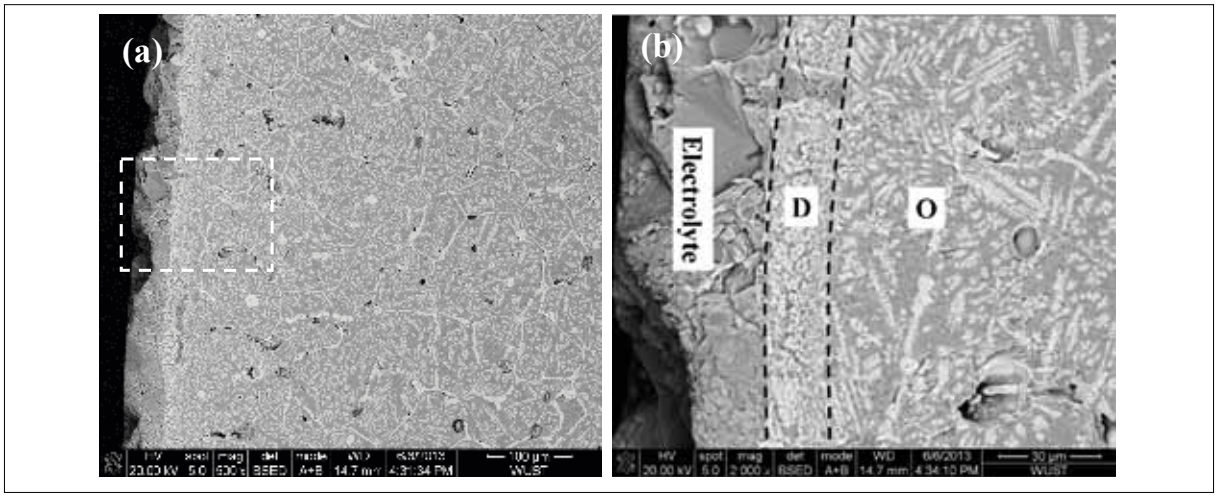

Fig. 5a–b SEM images of the corroded surface of specimen MTN30

electrolyte were mainly MgF_2 and Al_2O_3 [18]. In order to increase the corrosion resistance, high chemical substance $NiFe_2O_4$ or SnO_2 can be added into the composite. Moreover, TiO_2 can enhance densification magnesia materials [42], slowing down the penetration of electrolyte [24, 43]. Based on the above consideration, novel composites based on MgO–SnO_2–TiO_2 and MgO–$NiFe_2O_4$–TiO_2 systems for ledge-free sidewall were prepared and some experimental results were presented to demonstrate their sinterability and chemical stabilities in molten electrolyte in air.

4.1 MgO–$NiFe_2O_4$–TiO_2 system

The composition of the MgO-$NiFe_2O_4$-TiO_2 materials (labeled as MTN30) was 65 mass-% MgO, 30 mass-% $NiFe_2O_4$ and 5 mass % TiO_2. The XRD patterns (Fig. 4a) indicated that reaction between MgO and TiO_2 occurred to generate Mg_2TiO_4 that formed solid solution with $NiFe_2O_4$ to generate composite spinel ($Ni_\chi Ti_{1-\chi}Fe_{2\chi}Mg_{2-2\chi}O_4$) during sintering process, which promoted mass transfer and enhanced densification of the materials simultaneously (Fig. 4b). And light grey composite spinel distributed homogeneously in the matrix of the specimen.

The corroded SEM micrographs of MTN30 (Fig. 5a) revealed that no obvious corrosion phenomenon can be observed after 10 h immersion in electrolyte (57,8 mass-% K_3AlF_6-16,7 mass-% Na_3AlF_6-25,5 mass-% AlF_3) at 900 °C. And the dense layer (D) of 20 µm formed (Fig. 5b) that was indentified as solid-state solution of aluminates and $NiFe_2O_4$ by EDS analysis. The layer functions as the blocking layer between the origin layer (O) and electrolyte to improve the corrosion resistance [44].

Fig. 6 reveals phase evolution of 100 g MTN30 in electrolyte calculated by thermodynamic analysis software (FactSage 6.2). It can be seen that with increasing electrolyte content, MgO decreases continuously companying with the formation of fluorides and $MgAl_2O_4$ while no obvious changes can be found on the contents of $NiFe_2O_4$ and Mg_2TiO_4.

It indicated that $NiFe_2O_4$, Mg_2TiO_4 and their solid-state solution (the composite spinel) possessed better chemical stability than MgO in molten electrolyte.

4.2 MgO–SnO_2–TiO_2 system

The composition of the MgO-SnO_2-TiO_2 materials (labeled as MTS10) was 85 mass-% MgO, 10 mass-% SnO_2 and 5 mass-% TiO_2. XRD pattern of MTS10 (Fig. 7a) revealed that Mg_2SnO_4 and Mg_2TiO_4 formed and then solid solution $Mg_2Ti_xSn_{1-x}O_4$ during the heating process, which led to mass transfer and densification of the materials [45] (Fig. 7b).

The corroded SEM micrographs of MTS10 (Fig. 8a) presented that only a corrosion layer (C) of 30 µm formed at the surface of the specimen after 10 h test at 900 °C. And the elemental map of Al in Fig. 8b revealed that the infiltration of electrolyte was completely inhibited. It indicated that the MTS10 also demonstrated high corrosion resistance to the molten electrolyte, which was attributed to the lowering infiltration of electrolyte as well as high chemical stable composite spinel retarding chemical corrosion.

5 Outlook on the development of ledge-free sidewalls

The development of ledge-free sidewalls brings great economical and environmental opportunities in aluminum industry. Meantime, the sidewall materials are facing the critical challenge in service. The following issues of the research works need to be taken into consideration:

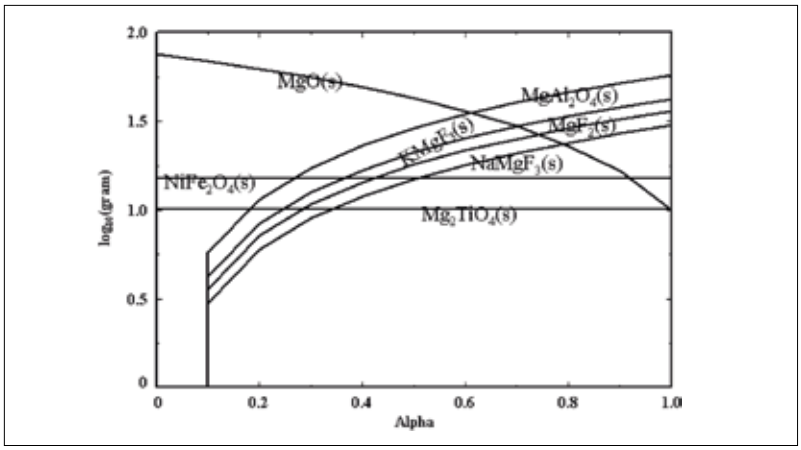

Fig. 6 predicted phase evolution of specimen MTN30 in the electrolyte at 900 °C

(1) New design for ledge-free sidewalls in aluminum cell is in need for selection criteria of sideling since a single material can hardly satisfy all the chemical requirements. Horizontal multi-layer strategy with two different materials is recommended, in which one of them can withstand the gas and bath zones while the other can withstand the bath and metal zones.

(2) $NiFe_2O_4$ and SnO_2 materials, candidates for inert anodes in aluminum reduction

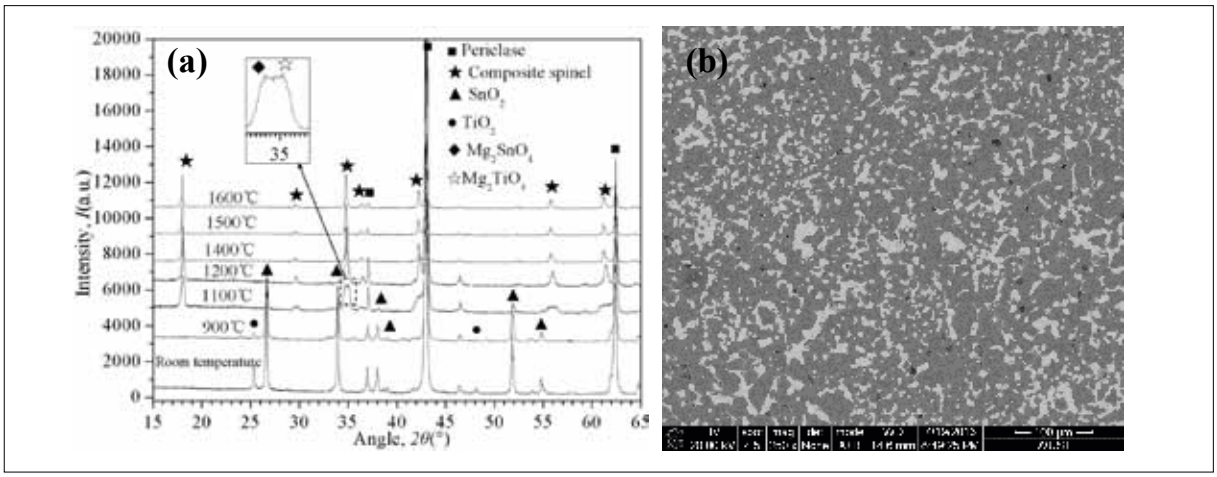

Fig. 7a–b XRD patterns of specimen MTS10 (a), and micrograph of specimen MTS10 fired at 1600 °C (b)

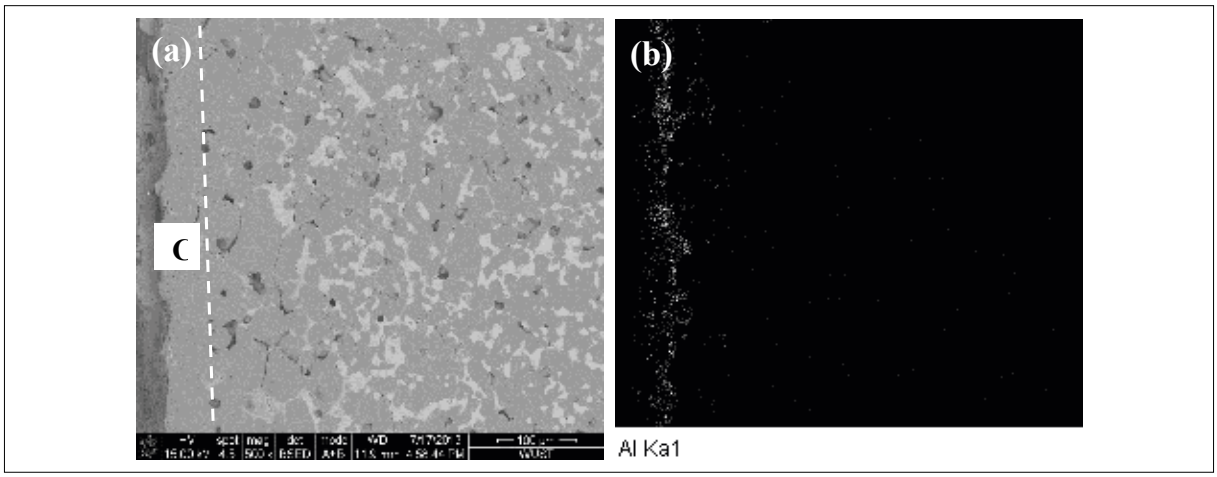

Fig. 8a–b SEM images of corroded specimen MTS10 (a), and elemental map of Al for the same region (b)

cell are also potential for the ledge-free sidewall in gas and bath zones. Furthermore, some aluminate spinel and composites containing high stability substances, e.g. $NiFe_2O_4$ and SnO_2, also deserve special attention since the price of pure $NiFe_2O_4$ and SnO_2 is too high to be used as sidewall materials.

(3) Issues relating to joining of materials, process control, manufacturing and maintenance also need to be addressed before new sidewall designs can be implemented.

References

[1] Grjotheim, K.; et al.: Aluminum smelter technology. Düsseldorf 1980

[2] Sonntag, A.; et al.: New R-SiC extends service life in kiln furniture. Amer. Ceram. Soc. Bull. **76** (1997) 51–54

[3] Wang, Z.; et al.: Spent Si_3N_4 bonded SiC sidelining materials in aluminum electrolysis cells. Light Metals (2009) 353–358

[4] Etzion, R.; et al.: Wear mechanism study of silicon nitride bonded silicon carbide refractory materials. Light Metals (2008) 955–958

[5] Thonstad, J.; et al.: Aluminum electrolysis. 3rd ed. Fundamentals of the Hall-Héroult process. Düsseldorf 2001

[6] Choate, W.T.; et al.: U.S. energy requirements for aluminum production: Historical perspective, theoretical limits and new opportunities. Energy efficiency and renewable energy. Washington, D.C., 2003

[7] Grjotheim, K.; et al.: Aluminum smelter technology. 2nd ed., Düsseldorf 1988

[8] Brooks, G.; et al.: Challenges in light metals production. Mineral Processing and Extractive Metallurgy **116** (2007) [1] 25–33

[9] Mukhlis, R.; et al.: Sidewall materials for Hall-Héroult process. Light Metals (2010) 883–888

[10] Yan, X.Y.; et al.: Aluminate spinels as sidewall linings for aluminum smelters. Light Metals. (2011) 1085–1090

[11] Nightingale, S.A.; et al.: Corrosion of nickel ferrite refractory by Na_3AlF_6–AlF_3–CaF_2–Al_2O_3 bath. J. Europ. Ceram. Soc. **33** (2013) 2761–2765

[12] Skybakmoen, E.; et al.: Chemical resistance of sidelining materials based on SiC and carbon in cryolitic melts – a laboratory study. Warrendale, PA (1999) 215–22.

[13] Mukhlis, R.Z.; et al.: Sidewall materials for Hall-Héroult process. High Temperature Processing, Swinburne University of Technology, Melbourne (2010) 63–66

[14] Kvande, H.; et al.: Inert anodes for Al smelters: Energy balances and environmental impact. JOM **53** (2001) [5] 29–33

[15] Welch, B.J.; et al.: Materials problem in Hall-Héroult cells. 8th Int. Leichtmetalltag, Leoben – Vienna (1987) 120–125

[16] Sadoway, D.R.: Inert anodes for the Hall-Héroult cell: the ultimate materials challenge. JOM **53** (2001) [5] 34–35

[17] Pownceby, M.I.: Literature review – materials for the sidewalls of Hall-Héroult cells. CSIRO Minerals, Clayton 2005

[18] Xu, Y.B.; et al.: Reaction between oxides and fluoride electrolyte at high temperature. Mat. Rev. **26** (2012) 106–111

[19] Pawlek, R.P.: Methods to test refractories against bath attack in aluminum electrolysis pots. Aluminum **70** (1994) 555–559

[20] Gao, B.L.; et al.: Corrosion tests and electrical resistivity measurement of SiC–Si_3N_4 refractory materials. Light Metals (2004) 419–424

[21] Zhao, J.G.; et al.: Test method for resistance of SiC material to cryolite. Light Metals (2006) 663–666

[22] Downie, K.: $NiFe_2O_4$ as a sidewall material in Hall-Héroult cells. Bachelor of Engineering Thesis, University of Wollongong, Wollongong, 2007

[23] Galasiu, I.; et al.: Inert anodes for aluminum electrolysis. Düsseldorf 2009

[24] Yan, X.Y.; et al.: Corrosion behaviour of nickel ferrite-based ceramics for aluminium electrolysis cells. Light Metals (2007) 909–913

[25] Sekhar, J.A.; et al.: Reduction conditions encountered in cryolite baths. Light Metals (1999) 383–387

[26] Olsen, E.; et al.: Nickel ferrite as inert anodes in aluminum electrolysis: Part I: Material fabrication and preliminary testing. J. Appl. Electrochem. **29** (1999) [3] 293–299

[27] Liu, B.; et al.: Electrical conductivity and molten salt corrosion behavior of spinel nickel ferrite. Solid State Sci. **13** (2011) [8] 1483–1487

[28] Bale, C.W.; et al.: FactSage thermochemical software and databases. Calphad **26** (2002) 189–228

[29] Xiao, H.; et al.: The solubility of SnO_2 in NaF-AlF_3-Al_2O_3 melts. Acta Chem. Scand. **49** (1995) 96–102

[30] Xiao, H.; et al.: Studies on the corrosion and the behavior of inert anodes in aluminum electrolysis. Metall. Mater. Trans. B. **27** (1996) [2] 185–193

[31] Liu, Y.X.; et al.: Oxygen overvoltage on SnO_2-based anodes in NaF–AlF_3–Al_2O_3 melts, electrocatalytic effects of doping agents. Electrochim. Acta **28** (1983) [1] 113–116

[32] Keller, R.; et al.: Mass transport considerations for the development of oxygen-evolving anodes in aluminum electrolysis. Electrochim. Acta **42** (1997) [12] 1809–1817

[33] Zuca, S.; et al.: Contribution to the study of SnO_2-based ceramics. J. Mat. Sci. **26** (1991) [6] 1673–1676

[34] Govorov, V.A.; et al.: $Sn_{2-2x}Sb_xFe_xO_4$ Solid solutions as possible inert anode materials in aluminum electrolysis. Chem. Mat. **17** (2005) [11] 3004–3011

[35] Popescu, A.M.; et al.: Microstructure and electrochemical behaviour of some SnO_2-based inert electrodes in aluminum electrolysis. J. Phys. Chem. **57** (2002) 71–75

[36] Vecchio-Sadus, A.M.; et al.: Tin dioxide-based ceramics as inert anodes for aluminium smelting: a laboratory study. Light Metals (1996) 259–265

[37] Popescu, A.M.; et al.: Structure and behaviour of ceramic materials based on SnO_2 used as inert anodes in electrowining processes. Rev. Roum. Chim. **55** (2010) [5] 319–328

[38] Jentoftsen, T.E.; et al.: Solubility of some transition metal oxides in cryolite-alumina melts: Part I. Solubility of FeO, $FeAl_2O_4$, NiO, and $NiAl_2O_4$. Metall. Mater. Trans. B. **3** (2002) 901–908

[39] Granfield, J.; et al.: The impact of rising Ni and V impurity levels in smelter grade aluminum and potential control strategies. Mater. Sci. Forum **630** (2010) 129–136

[40] Othman, A.G.M.: Effect of talc and bauxite on sintering, microstructure, and refractory properties of Egyptian dolomitic magnesite. Br. Ceram. Trans. **102** (2003) [6] 265–271

[41] Liu, Y.X.; et al.: Modern aluminum electrolysis. Beijing 2008

[42] Lee, Y.B.; et al.: Sintering and microstructure development in the system MgO-TiO_2. J. Mater. Sci. **33** (1998) [17] 4321–4325

[43] Li, J.; et al.: Effect of NiO content on corrosion behaviour of Ni–xNiO–$NiFe_2O_4$ cermets in Na_3AlF_6–Al_2O_3 melts. T. Nonferr. Metal. Soc. **14** (2004) [6] 421–425

[44] Liu, J.Y.; et al.: Phase evolution of 17(Cu-10Ni)-($NiFe_2O_4$–10NiO) cermet inert anode during aluminum electrolysis. T. Nonferr. Metal. Soc. **21** (2011) [3] 566–572

[45] Azad, A.M.: Mg_2SnO_4 ceramics I. Synthesis- processing-microstructure correlation. Ceram. Int. **27** (2001) 325–334